

**SCALAR SYNCHROTRON RADIATION IN THE
SCHWARZSCHILD-ANTI-DE SITTER GEOMETRY**

Vitor Cardoso

CENTRA, Departamento de Física, Instituto Superior Técnico,
Av. Rovisco Pais 1, 1096 Lisboa, Portugal,
E-mail: vcardoso@fisica.ist.utl.pt

José P. S. Lemos

CENTRA, Departamento de Física, Instituto Superior Técnico,
Av. Rovisco Pais 1, 1096 Lisboa, Portugal,
&
Institute of Astronomy, University of Cambridge,
Madingley Road, CB3 0HA, Cambridge, UK
E-mail: lemos@kelvin.ist.utl.pt**Abstract**

We present a complete relativistic analysis for the scalar radiation emitted by a particle in circular orbit around a Schwarzschild-anti-de Sitter black hole. If the black hole is large, then the radiation is concentrated in narrow angles- high multipolar distribution- i.e., the radiation is synchrotronic. However, small black holes exhibit a totally different behavior: in the small black hole regime, the radiation is concentrated in low multipoles. There is a transition mass at $M = 0.427R$, where R is the AdS radius. This behavior is new, it is not present in asymptotically flat spacetimes.

1 Introduction

Cyclotron and synchrotron radiations both have inherited their names from the apparatus used to accelerate charged particles in the 30's and 40's of last century. The radiation generated due to the charge acceleration was a secondary effect which became a subject on itself. Cyclotron radiation comes from electrically charged particles in a magnetic field \vec{B} with non-relativistic velocities \vec{v} in circular or spiralling (along \vec{B}) orbits, which spectrum consists of a single frequency of emission, equal to the orbital frequency of the particle in the magnetic field, $\omega_0 = 2\pi\frac{qB}{m}$, where q and m are the charge and mass of the particles, respectively. For highly relativistic particles the spectrum is much more complex and most of the power is radiated in a range around a frequency $\bar{\omega}$, which is many times the orbital particle frequency ω_0 , $\bar{\omega} \simeq \gamma^3\omega_0$, where gamma is the Lorentz factor, into a narrow cone due to relativistic headlight effect, and strongly linearly polarized in the plane of the circular motion. This radiation due to relativistic circular particles is called synchrotron radiation. There is of course a transition from cyclotron to synchrotron radiation, in which the particle acquires larger and larger velocities and higher and higher harmonics of the fundamental mode ω_0 start to be excited. Instead of receiving a sinusoidal pulse with a sharp frequency as in the cyclotron radiation case, the observer starts to receive a series of sharp pulses repeating at intervals of $2\pi/\omega_0$. Synchrotron radiation is an important electromagnetic radiation in astrophysical systems such as the Sun, the magnetosphere of Jupiter, pulsars, and active galaxies (for detailed analysis of synchrotron radiation see [1, 2]). Fields other than the electromagnetic (vector) field, like the scalar [3] and the gravitational (tensorial) field [4], can also radiate synchrotronically in flat spacetime. The spectrum has for the three fields the form $P(\omega) \propto \omega \exp(-2\omega/\omega_{\text{crit}})$, with ω_{crit} being a few times $\bar{\omega}$.

By using the equivalence principle, one can further ask whether it is possible for a particle in geodesic motion in a gravitational field to emit cyclotron or synchrotron radiation. Indeed, cyclotron gravitational radiation has been studied, see, e.g., [5] for recent work on detailed calculations of gravitational radiation from a particle in a geodesic circular orbit around a Schwarzschild black hole, which is motivated mainly by the possibility of detecting gravitational waves by LIGO or VIRGO projects. On the other

hand, Misner et al [6, 7] showed that geodesic synchrotron radiation (GSR) is possible for particles near the relativistic photonic orbits around a black hole. This radiation was first worked out for scalar particle and field in a Schwarzschild black hole [7] and it showed three main features: (i) the range of radiated frequencies $\bar{\omega}$ are higher harmonics (or higher multipoles) of the particle's orbital frequency $\omega_0 = (M/r_0^3)^{1/3}$, namely, $\bar{\omega} \simeq \gamma^2 \omega_0$, where γ is the Lorentz factor, $\gamma = 1/\sqrt{1 - 3M/r_0}$, and M and r_0 are the mass of the black hole and the position of the orbit, respectively, (ii) it is beamed into narrow orbital plane angles, and (iii) it is linearly polarized in the orbital plane [8]. The existence of GSR was then studied for electromagnetic and gravitational fields [9] where it was shown that the spectrum is broader than for the scalar field, $P(\omega) \propto \omega^{1-s} \exp(-2\omega/\omega_{\text{crit}})$, with s being the spin of the radiated field, and again ω_{crit} being a few times $\bar{\omega}$. It is interesting to note, following [10], that there are differences between ordinary (or accelerated) synchrotron radiation (OSR) and GSR. For OSR the spectrum does not depend on the spin s of the field, whereas for GSR it does. This stems from the fact that geometric optics (short wavelength approximation) is valid for a source in flat spacetime, whereas in a strong gravitational field the effective gravitational potential does not permit short waves within the emitting region [10]. GSR went into oblivion after it was shown that the GSR concept was not applicable astrophysically [11, 12], mainly due to the fact that it is astrophysically hard to put particles on photonic orbits, although some attempts with non-geodesic motion were made [13].

However, black holes are now not only of astrophysical interest but also are of interest to elementary particle physics. Since many elementary particle theories predict that the vacuum is anti-de Sitter (AdS) one should reanalyze the problem in a Schwarzschild-AdS background and work out the similarities and the differences. This is what we do in this paper. In this paper we shall study a specific important problem of radiation emission: the scalar energy emitted by a small test particle coupled to a massless scalar field as it orbits in circular motion a Schwarzschild-AdS black hole. This work is then also of interest to the AdS/CFT conjecture [14], which in turn has attracted much attention to the investigation of asymptotically AdS spacetimes. According to it phenomena in the bulk can be reinterpreted as phenomena in the Conformal Field Theory (CFT) boundary. In addition, the black hole corresponds to a thermal state in the conformal field theory, and the decay

of a test field in the black hole spacetime, correlates to the decay of the perturbed state in the CFT. One knows for example that the decay of this test field is correctly described by the so called quasinormal modes, which have been recently computed for AdS spacetimes (see, e.g. [16], and references therein). In order to gain deeper insight into the conjecture, one needs to understand how the information about the bulk is encoded in the boundary, namely by probing the bulk with test fields, or pointlike particles [17], and to understand how the spacetime answers to specific perturbations. A specific problem, the radial infall of a small test particle into a Schwarzschild-AdS black hole and consequent emission of radiation is being addressed [18], where it is found that the signal is dominated by quasinormal ringing (for the analogous problem in the BTZ 3-dimensional black hole see [19]).

The paper is organized as follows. In section 2 , we introduce the problem, and the basic mathematical apparatus needed to solve it. In section 3 , we present the numerical results obtained, and the most important features of these numerical results. In section 4 , we present some concluding remarks.

2 Equations and Formalism

2.1 The problem

Black holes in AdS spacetimes in several dimensions have been recently study. All dimensions up to eleven are of interest in superstring theory, but experiment singles out four dimensions (4D) as the most important. In 4D general relativity, an effective gravity theory in an appropriate string theory limit, the Kerr-Newman family of four-dimensional black holes can be extended to include a negative cosmological constant [20]. Our background is the 4D Schwarzschild-AdS black hole metric,

$$ds^2 = f(r)dt^2 - \frac{dr^2}{f(r)} - r^2(d\theta^2 + \sin^2 \theta d\phi^2), \quad (1)$$

where, $f(r) = (\frac{r^2}{R^2} + 1 - \frac{2M}{r})$, R is the AdS radius and M the black hole mass. We now consider a small particle coupled to a massless scalar field,

described by the interaction action [7]

$$S = -\frac{1}{8\pi} \int g^{1/2} \varphi_{;a} \varphi^{;a} d^4x - m_0 \int (1 + q_s \varphi) (-g_{ab} \dot{z}^a \dot{z}^b)^{1/2} d\lambda, \quad (2)$$

where q_s is the scalar charge carried by the test particle, and m_0 its mass. The mass m_0 is supposed to be small and the scalar field treated as a perturbation, in the sense that the background metric is still given by (1). This means that the particle travels on a geodesic of the spacetime.

After the usual decomposition in spherical harmonics, $\varphi(r, \omega, \theta, \phi) = \frac{1}{r} \sum_{lm} \psi(r, \omega) Y_{lm}$, where Y_{lm} are the usual spherical harmonics, and a Fourier transform $\Psi(r, \omega) = \frac{1}{(2\pi)^{1/2}} \int_{-\infty}^{\infty} e^{i\omega t} \psi(r, t) dt$, the evolution of the scalar field is given by the wave equation with a generic source term S :

$$\frac{\partial^2 \Psi(r)}{\partial r_*^2} + [\omega^2 - V(r)] \Psi(r) = S. \quad (3)$$

Here,

$$S = \int \frac{1}{(2\pi)^{1/2}} \frac{f(r)}{\gamma r} Y_{lm}(\theta, \phi) e^{i\omega t} \delta(r - r(t)) dt, \quad (4)$$

where $r(t)$, $\theta(t)$ and $\phi(t)$ are the spatial Schwarzschild coordinates of the test particle, and $\gamma = 1/\sqrt{1 - 3M/r}$. The potential V appearing in equation (3) is given by

$$V(r) = f(r) \left[2 + \frac{2M}{r^3} + \frac{l(l+1)}{r^2} \right]. \quad (5)$$

The tortoise coordinate r_* is defined as $\frac{\partial r}{\partial r_*} = f(r)$.

2.2 Circular geodesics in the Schwarzschild-AdS geometry

Since to the best of our knowledge, no full investigation has been made on the geodesics in this spacetime, we shall study the circular null and timelike geodesics in the Schwarzschild-AdS geometry, which will be useful in what follows. The integrals of motion $f dt/d\tau = E$, and $r^2 d\phi/d\tau = L$, where E is an energy parameter and L an angular momentum parameter, plus the constancy of the Lagrangian yield

$$\dot{r}^2 + V(r)^2 = E; \quad V(r)^2 = f(\epsilon + L^2/r^2), \quad (6)$$

where $\epsilon = 0$ for null geodesics and $\epsilon = 1$ for timelike geodesics.

(i) Timelike circular geodesics: in this case $\epsilon = 1$. Demanding $dV^2/dr = 0$ we get

$$L^2 = \frac{r^5/R^2 + Mr^2}{r - 3M}, \quad (7)$$

and

$$\omega_0 \equiv d\phi/dt = \left(\frac{1}{R^2} + \frac{M}{r^3}\right)^{1/2}. \quad (8)$$

This means that circular timelike geodesics may exist for any $3M < r < \infty$. Let us now see which of them are stable and which are unstable. If we differentiate twice the potential and then substitute L^2 given by (7), we obtain

$$d^2V^2/dr^2 = -2\frac{15Mr^3 - 4r^4 + 6M^2R^2 - MR^2r}{r^3R^2(r - 3M)}. \quad (9)$$

Now, (9) has one and only one real root in $3M < r < \infty$. This root will give us the range of allowed stable and unstable circular orbits. The roots can be done numerically, but two important limiting cases can be studied analytically, and these are the very large and very small black hole limit. For very large black holes, we can immediately see that the root is at $r = 15/4M = 3.75M$. For very small black holes we can see that the root is at $r = 6M$, which is what we expect: for small black holes the results of the Schwarzschild geometry should carry over. For any intermediate mass, the last stable circular orbit lies in between $r = 3.75M$ and $r = 6M$.

(ii) Null circular geodesics: in this case we require $\epsilon = 0$, $\dot{r} = 0$ and $dV^2/dr = 0$, which gives us

$$r = 3M; \quad \frac{E^2}{L^2} = \frac{1}{R^2} + \frac{1}{27M^2}, \quad (10)$$

and $d^2V^2/dr < 0$. Thus, just as in Schwarzschild spacetime, a circular orbit of radius $3M$ is the only allowed null geodesic, which is furthermore an unstable one.

2.3 The Green's function solution

Under these conditions, (3) becomes

$$\frac{\partial^2 \Psi(r)}{\partial r_*^2} + [m^2 \omega_0^2 - V(r)] \Psi(r) = S_l \delta(r - r_0), \quad (11)$$

with $S_l = 4f(r)\pi Y_{lm}(\pi/2, 0)/(\gamma r)$, and again $\gamma = 1/\sqrt{1 - 3M/r_0}$. We would like to draw attention to the fact that for circular geodesic motion the frequency ω must be a multiple of the frequency ω_0 of revolution around the black hole, i.e., $\omega = m\omega_0$. In (11) we have rescaled r , $r \rightarrow \frac{r}{R}$, and measure everything in terms of R , i.e., ω is to be read ωR , Ψ is to be read $\frac{R}{q_s m_0} \Psi$ and r_+ , the horizon radius is to be read $\frac{r_+}{R}$. Equation (11) is to be solved under the boundary conditions appropriate for Schwarzschild-AdS black holes: ingoing waves at the horizon ($\Psi \sim Ae^{-i\omega r_*}$), and reflective boundary conditions ($\Psi = 0$) at infinity [21]. Of course, under these conditions, all the energy eventually goes down the black hole, and this is the energy we are interested in compute. To implement a numerical solution, we note that two independent solutions Ψ_1 and Ψ_2 of (11), with the source term set to zero, have the behavior:

$$\Psi_1 \sim e^{-i\omega r_*}, r \rightarrow r_+ \quad (12)$$

$$\Psi_1 \sim Ar + B/r^2, r \rightarrow \infty \quad (13)$$

$$\Psi_2 \sim 1/r^2, r \rightarrow \infty \quad (14)$$

$$\Psi_2 \sim Ce^{i\omega r_*} + De^{-i\omega r_*}, r \rightarrow r_+ \quad (15)$$

The Wronskian of these two solutions is $W = 2Ci\omega$. By a standard Green's function analysis, we get that the solution to the inhomogeneous equation (11) behaves, near the horizon, as

$$\Psi = \frac{e^{-i\omega r_*}}{(2i\omega C)} \int_{r_+}^{\infty} \frac{S\Psi_2}{f} \delta(r - r_0) dr \quad (16)$$

$$= \frac{e^{-i\omega r_*}}{(2i\omega C)} \frac{S}{f}(r_0) \Psi_2(r_0). \quad (17)$$

All we need to do is find a solution Ψ_2 of the corresponding homogeneous equation satisfying the above mentioned boundary conditions (15). In the

numerical work, we chose to adopt r as the independent variable, therefore avoiding the numerical inversion of $r_*(r)$. The integration was started at a large value of $r = r_i$, which was $r_i = 10^5 r_+$ typically. Equation (15) was used to infer the boundary conditions $\Psi_2(r_i)$ and $\Psi'_2(r_i)$. We then integrated inward from $r = r_i$ into typically $r = r_+ + 10^{-6} r_+$. Equation (15) was then used to get C .

The total power P_{tot} radiated into the black hole is $P_{\text{tot}} = \sum_{l,m>0} \frac{\omega^2}{2\pi} |\Psi|^2$, and the power spectra P (power radiated at a given frequency $\omega = m\omega_0$) is

$$P(m\omega_0) = \sum_{l \geq |m|} \frac{(m\omega_0)^2}{2\pi} |\Psi|^2 \quad (18)$$

where m is fixed in the summation.

3 Numerical results

3.1 Large and intermediate black holes

We define large and intermediate black holes as black holes with $r_+ \geq 1$. The results of the numerical integration are shown in Figures 1a and 1b for orbits at $r_0 = 5$ and $r_0 = 20$, respectively, and a horizon radius $r_+ = 1$. In Figure 2 it is shown the power spectra as a function of the azimuthal quantum number m for large m in a semi-log plot.

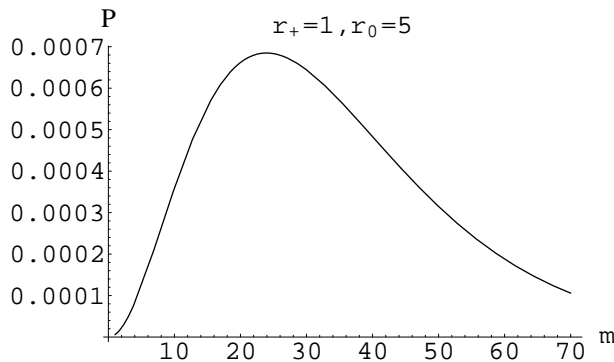


Figure 1a. Scalar radiation power spectra as a function of the azimuthal quantum number m , for an orbit with $r_0 = 5$, around a Schwarzschild-AdS black hole with $r_+ = 1$.

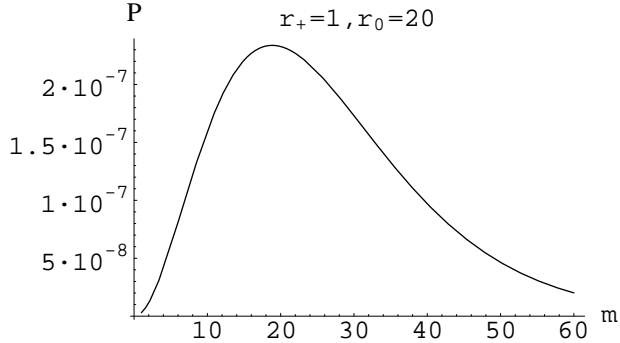


Figure 1b. Scalar radiation power spectra as a function of the angular quantum number m , for an orbit with $r_0 = 20$, around a Schwarzschild-AdS black hole with $r_+ = 1$.

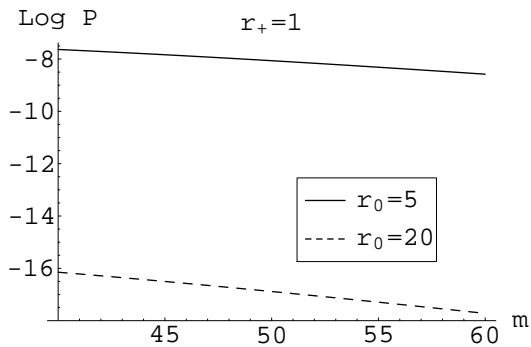


Figure 2. Plot of $\log P \times m$ for large m . One can see that $\log P$ is a linear function of m , so that for large m the power output decreases exponentially.

The results for the large black hole regime are the following:

- (1) The power radiated in the $l = m$ modes is more than 95% of the total power.
- (2) High multipoles, as one can see from Figs. 1a and 1b, are clearly enhanced, and the radiation is synchrotronic. To see that most of the radiation is in fact confined to small angles, we have plotted the angular distribution of the power in Fig. 3.
- (3) The location of the peak of the spectrum increases with increasing radius of the circular orbit, so that truly synchrotronic radiation occurs only for highly relativistic (unstable) orbits.
- (4) From Figs. 1a and 1b, and as expected, we see that the power output decreases with increasing r_0 , the orbit radius. In fact one can easily prove that for high r_0 the power goes as $1/r_0^6$.

(5) The location of the peak increases dramatically with the mass of the hole. So for large black holes the emission is dominated by very large m . This strong dependence of the location of the peak on the black hole mass, makes us believe that small black holes do not emit synchrotronic radiation. This will be seen to be true in the next subsection.

(6) Furthermore, the power decays as an exponential power of the frequency, for high frequencies, which is evident from Fig. 2, where we show a plot of $\log P \times m$; An analytical approximation for large m seems very difficult to achieve, due to the behavior of the potential. We find numerically that for large m , the exponential dependence of the power spectra is

$$P \sim e^{-\frac{2\omega}{\omega_{\text{crit}}}} \quad (19)$$

where $\omega_{\text{crit}} = \frac{2\gamma M^2 \omega_0}{0.09}$. We conclude from this that most of the radiation is emitted at a given $\bar{\omega}$ and that $\bar{\omega}$ increases with the mass of the black hole (numerically we have found $\bar{\omega} \sim M^2$).

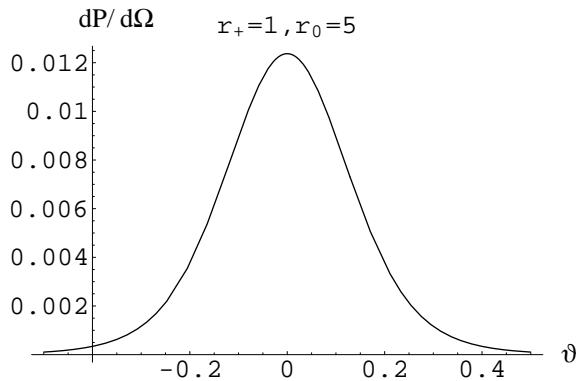


Figure 3. Scalar power per unit solid angle $\vartheta \equiv \pi/2 - \theta$, for the case of a scalar particle orbiting around a $r_+ = 1$ black hole, with an orbital radius $r_0 = 5$.

3.2 Small black holes

In Figs. 4a and 4b we show the numerical results for small black holes, $r_+ < 1$.

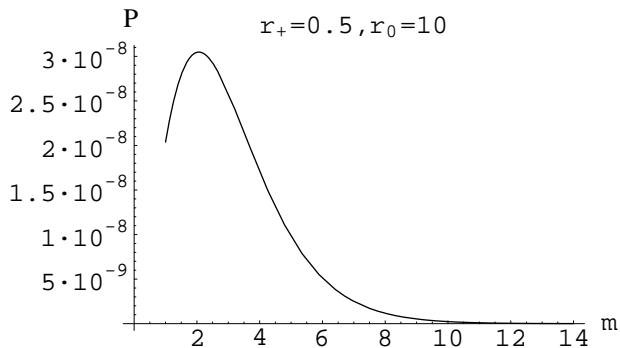


Figure 4a. Scalar radiation power as a function of the angular quantum number m , for an orbit with $r_0 = 10$, around a Schwarzschild-AdS black hole with $r_+ = 0.5$.

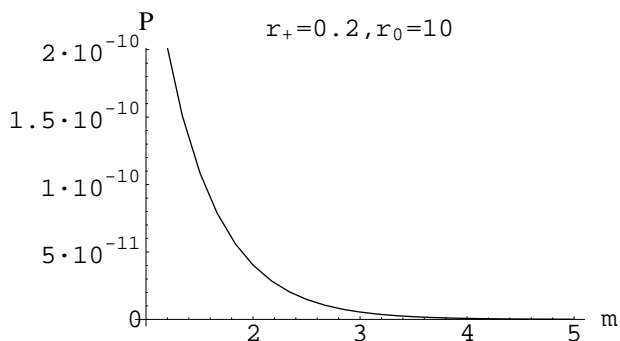


Figure 4b. Scalar radiation power as a function of the angular quantum number m , for an orbit with $r_0 = 10$, around a Schwarzschild-AdS black hole with $r_+ = 0.2$.

In the small black hole regime, we can see a completely different behavior, in that now the power decreases monotonically with m , the angular quantum number. Numerically, we find that, independently of r_0 , the location (in l) of the peak of the spectrum progressively approaches $m = 0$ as one lowers the mass of the black hole. Finally, for $M < 0.427R$ ($r_+ < 0.618R$) the spectrum is monotonically decreasing in m , for all m . Still, for large m the spectrum continues to decay exponentially.

3.3 Conclusions

We have computed the scalar radiation emitted by a scalar test particle moving in a geodesic circular orbit around a Schwarzschild-AdS black hole. For large black holes, the radiation is confined to small angles, and we therefore have what can be

called scalar synchrotron radiation. However, the spectrum depends drastically on the size of the black hole. For black holes with masses $M < 0.427R$ the spectrum does not have a peak in m , and so in this regime there is no synchrotron radiation. One might be tempted at first sight to say that small black holes in AdS spacetime should behave like Schwarzschild black holes. Our numerical results show that this is not true: the boundary conditions at infinity have changed.

These results, plus results on all previously mentioned works on AdS spacetime, allows us to slowly start building a small catalog of dynamical processes in AdS spacetimes. It's worth emphasizing that this is extremely important if one wants to fully understand the AdS/CFT duality and whatever surprises there may be to unfold in AdS spaces. Indeed here, in relation to the AdS/CFT correspondence, one can say that to the black hole corresponds a thermal bath, to the orbiting particle corresponds a travelling soliton (lump of energy), and to the scalar field waves correspond particles decaying into bosons of the associate operator of the gauge theory. Thus in the CFT boundary one has a travelling soliton perturbing the thermal state and irradiating particle pairs [15].

Acknowledgments

This work was partially funded by Fundação para a Ciência e Tecnologia (FCT) through project SAPIENS 36280. VC also acknowledges financial support from FCT through PRAXIS XXI programme. JPSL thanks Observatório Nacional do Rio de Janeiro for hospitality. We thank conversations with Donald Lynden-Bell.

References

- [1] J. D. Jackson, *Classical Electrodynamics*, (J. Wiley, New York 1975).
- [2] G. B. Rybicky, A. P. Lightman, *Radiative Processes in Astrophysics*, (J. Wiley, New York 1979).
- [3] R. A. Breuer, in *Gravitational Perturbation Theory and Synchrotron Radiation*, (Springer Lect. Notes in Physics, no 44).
- [4] R. H. Price, V. D. Sandberg, *Phys. Rev. D* **8**, 1640 (1973).
- [5] E. Poisson, *Phys.Rev. D***52**, 5719 (1995);
- [6] C. W. Misner, *Phys. Rev. Lett.* **28**, 994 (1972).

- [7] C. W. Misner, R. A. Breuer, D. R. Brill, P. L. Chrzanowski, H. G. Hughes III, and C. M. Pereira, *Phys. Rev. Lett.* **28**, 998 (1972); R. A. Breuer, P. L. Chrzanowski, H. G. Hughes III, C. W. Misner, *Phys. Rev. D* **8**, 4309 (1973).
- [8] R. A. Breuer, C. V. Vishveshwara, *Phys. Rev. D* **7**, 1008 (1973).
- [9] R. A. Breuer, R. Ruffini, J. Tiomno, C. V. Vishveshwara *Phys. Rev. D* **7**, 1002 (1973).
- [10] D. M. Chitre, R. H. Price, *Phys. Rev. Lett.* **29**, 185 (1972).
- [11] M. Davis, R. Ruffini, J. Tiomno, F. Zerilli, *Phys. Rev. Lett.* **28**, 1352 (1972).
- [12] J. M. Bardeen, W. H. Press, S. A. Teukolsky, *Astroph. J.* **178**, 347 (1972).
- [13] A. N. Aliev, D. V. Galtsov, *Gen. Rel. Grav.* **13**, 899 (1981).
- [14] J. M. Maldacena, *Adv. Theor. Math. Phys.* **2**, 253 (1998).
- [15] O. Aharony, S. S. Gubser, J. Maldacena, H. Ooguri, Y. Oz, *Phys. Rept.* **323**, 183 (2000).
- [16] S. F. J. Chan and R. B. Mann, *Phys. Rev. D* **55**, 7546 (1997). G. T. Horowitz, V. Hubeny, *Phys. Rev. D* **62**, 024027 (2000); V. Cardoso, J. P. S. Lemos, *Phys. Rev. D* **64**, 084017 (2001).
- [17] O. Aharony, S. S. Gubser, J. Maldacena, H. Ooguri, Y. Oz, *Phys. Rept.* **323**, 183 (2000); I. R. Klebanov, “TASI Lectures: Introduction to the AdS/CFT Correspondence”, hep-th/0009139; E. Witten, *Adv. Theor. Math. Phys.* **2**, 253 (1998); U. H. Danielsson, E. Keski-Vakkuri, M. Kruczenski, *Nucl. Phys. B* **563**, 279 (1999); *JHEP* **0002**, 039 (2000).
- [18] V. Cardoso, J. P. S. Lemos, in preparation (2002).
- [19] V. Cardoso, J. P. S. Lemos, submitted (2001), hep-th/0112254.
- [20] B. Carter, “General theory of stationary black hole states”, in *Black Holes*, eds B. DeWitt, C. DeWitt, (Gordon Breach, New York 1973).
- [21] S. J. Avis, C. J. Isham and D. Storey, *Phys. Rev. D* **18**, 3565 (1978).
- [22] V. P. Frolov, and I. D. Novikov, in *Black Hole Physics - Basic Concepts and New Developments*, (Kluwer Academic Publishers, 1998).